

Research on bridgeless PFC circuit control algorithm of electric vehicle charging pile

HONGLAI YAN¹

Abstract. In order to solve the problem of input voltage instability and output load fluctuation when the electric vehicle charging pile is charging the charging pile, the bridgeless power factor correcting (PFC) control algorithm of charging pile as the research object is taken, and made a detailed analysis and research. Firstly, the mathematical model of bridgeless PFC circuit is established, and the commonly used single cycle control algorithm is deduced. According to the theory, the simulation model of bridgeless PFC is established. According to the test data of simulation circuits in input voltage disturbance, output voltage fluctuation, power factor and other aspects, the algorithm is used as a control algorithm for the circuit, and the simulation verification is carried out on it.

Key words. Electric vehicle, bridgeless PFC, single cycle control algorithm.

1. Introduction

With the progress of science and technology and development of economy, the vehicle has become an indispensable means of transport in people's lives. At the same time, the energy and environmental problems caused by traditional vehicles are becoming more and more serious. In order to solve the energy and environmental problems, pure electric vehicles began to be widely promoted [1, 2]. With the increase in pure electric vehicles, the charging behavior of a large number of pure electric vehicles has a great impact on the power grid [3].

From the load point of view, charging pile is a harmonic source load. When the pure electric vehicle is charging through the charging pile, the charging pile injects the harmonic current into the grid, thus affecting the quality of the current and voltage in the grid. With a large number of pure electric vehicles entering the market, when a region has a large number of charging piles that charge purely electric vehicles, it leads to regional load fluctuations of the grid, which will also influence the power supply voltage of the grid. The floating of the grid voltage

¹Xi'an International University, Shaanxi, 710000, China

adversely affects the battery life of a pure electric vehicle which is charged through the charging pile. At the same time, the power conversion circuit of the charging pile inevitably produces electromagnetic interference in the course of work. The presence of electromagnetic interference not only has a great impact on the sensitive electronic equipment (meters, etc.) of the charging pile, but undesirable components of current also penetrate into the power grid and cause harmonic pollution. The battery model of the pure electric vehicle is different, and when the same battery is charged in different power conditions, the load will exhibit some differences. The existence of these problems makes the power conversion circuit of the charging pile need to have a good anti-interference barrier to the input voltage and output load fluctuations, and need to meet the electromagnetic compatibility in the normal operation process.

2. Methods

2.1. Analysis of the circuit model of bridgeless Boost PFC

The boost power factor correcting (Boost PFC) circuit has many kinds of structures [4, 5] at present, because the two switch tubes and the diode in the Boost PFC circuit are the same model. Especially, when the bridgeless Boost PFC uses two independent inductances, it needs to keep the inductance of the two inductors the same. Therefore, the bridgeless Boost PFC equivalent circuit can be expressed in a uniform form, that is, it can be equivalent to the combination of two Boost PFC which take turns to work when the frequency input voltage is in the positive and negative two-half cycles. In order to combine the circuit to analyze, the bridgeless Boost PFC in this paper is taken as an example to analyze the circuit. The analysis process and results of the bridgeless Boost PFC circuit can be applied to other topologies.

2.1.1. Large-signal model of bridgeless Boost PFC. Before the analysis of the bridgeless Boost PFC circuit the following assumptions need to be made:

1. All the semiconductor devices in the circuit are regarded as ideal device.
2. The bridgeless Boost PFC circuit works in continuous conduction mode (CCM mode).
3. Switching frequency is far higher than the frequency of AC input voltage

According to the analysis of two modes of Boost PFC circuit, the equivalent of Boost PFC is obtained. The circuit is shown in Fig. 1.

The equivalent circuit shown in Fig. 1 can be divided into two different operating states according to the turn-off of the switch S. According to the switch tube conduction and shutdown, the flow direction analysis of the voltaic is shown in Fig. 2, which is the equivalent circuit of the bridgeless Boost PFC in a cycle.

When the switch tube S is in the conduction, the state equation of the inductor current and capacitance voltage in the circuits under the condition of the breakover can be obtained according to the Kirchhoff's theorems:

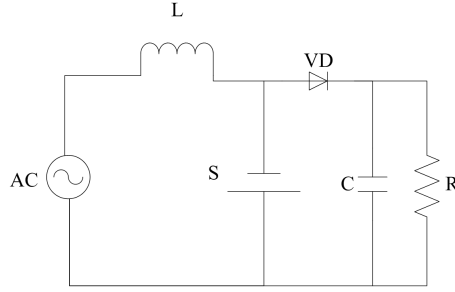


Fig. 1. Equivalent circuit of bridgeless Boost PFC

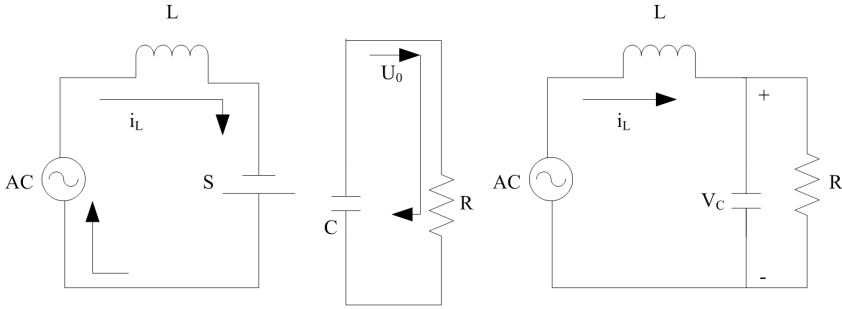


Fig. 2. Equivalent circuit of bridgeless Boost PFC in one cycle

$$\frac{di_L}{dt} = -\frac{1}{L}V_c, \quad (1)$$

$$\frac{dV_c}{dt} = -\frac{1}{RC}V_c, \quad (2)$$

where i_L is the input inductor current and V_c is the output capacitor voltage. When the switch tube is off, the state equations of the input inductor and capacitor voltage can be obtained in the form

$$\frac{di_L}{dt} = -\frac{1}{L}V_c + \frac{1}{L}v_{ac}, \quad (3)$$

$$\frac{dV_c}{dt} = \frac{1}{C}i_L - \frac{1}{RC}V_c. \quad (4)$$

Since it is assumed that the switching frequency is much greater than the frequency of the AC power, the input voltage U_{in} in the switching cycle is a fixed value. When the bridgeless Boost PFC is in the CCM mode, it is assumed that the duty cycle of the switch tube is d , the break duty cycle is d' , the input inductor current

i_L and the output capacitor voltage V_C are the state quantities for each switching cycle. The state equation for a switching period is given as

$$\begin{aligned} \begin{pmatrix} i_L^g \\ v_C^g \end{pmatrix} &= d \left(\begin{pmatrix} 0 & 0 \\ 0 & \frac{1}{RC} \end{pmatrix} \cdot \begin{bmatrix} i_L \\ v_C \end{bmatrix} + \begin{bmatrix} \frac{1}{L} \\ 0 \end{bmatrix} \cdot U_{in} \right) + \\ &+ d' \left(\begin{pmatrix} 0 & -\frac{1}{L} \\ \frac{1}{C} & -\frac{1}{RC} \end{pmatrix} \cdot \begin{bmatrix} i_L \\ v_C \end{bmatrix} + \begin{bmatrix} \frac{1}{L} \\ 0 \end{bmatrix} \cdot U_{in} \right). \end{aligned} \quad (5)$$

Assuming that $v_s(t)$ represents the voltage of the both ends of the switch tube, $i_D(t)$ is the current flowing through the diode D in the figure. In order to facilitate the analysis, the output voltage is expressed with $U_{in} = 1$. Since the uncontrollable rectifier bridge is eliminated in bridgeless PFC circuit, the input inductance is directly connected to the output side. The inductor current $i_L(t)$ and output current $i_0(t)$ is equal. Therefore, we can get the large signal expression between the mean current $i_D(t)$ across the diode and the voltage $v_s(t)$ of the both ends of the switch tube in a complete cycle:

$$v_s(t) = d'(t)U_0(t), \quad (6)$$

$$i_D(t) = d'(t)i_0(t). \quad (7)$$

2.1.2. Small-signal analysis of Boost PFC without bridge. In the process of bridgeless Boost PFC working, each system variable contains steady-state variables and perturbation components. Assuming that the voltage of the both ends of the switch tube S is $v_s(t)$ and output voltage is $v_0(t)$, the current of diode D is $i_D(t)$, the input current is $i_g(t)$, the steady-state components of the power switch tube S in off duty cycle $d'(t)$ are U_0, V_s, I_D, I_g, D' and the disturbance components can be expressed as $\hat{v}_s, \hat{v}_0, \hat{i}_D, \hat{i}_g, \hat{d}'$, the formulae (6)–(7) can be written as

$$v_s + \hat{v}_s = D'(U_0 + \hat{v}_0) + \hat{d}'(U_0 + \hat{v}_0), \quad (8)$$

$$i_D + \hat{i}_D = D'(I_g + \hat{i}_g) + \hat{d}'(I_g + \hat{i}_g). \quad (9)$$

Because the disturbance quantity of the circuit is set to be small, so $\hat{d}'\hat{v}_0$ and $\hat{d}'\hat{i}_g$ can be neglected. The small signal expressions (10) and (11) of the voltage $v_s(t)$ and the current $i_D(t)$ can be obtained.

$$\hat{v}_s = D'\hat{v}_0 + \hat{d}'V_0, \quad (10)$$

$$\hat{i}_D = D'\hat{i}_g + \hat{d}'I_g. \quad (11)$$

From the small signal model of the voltage $v_s(t)$ and current $i_D(t)$, the frequency

domain expression in the circuit can be obtained in the form

$$\hat{v}_g(s) = U_0 \hat{d}'(s) + D' \hat{v}(s) + SL \hat{i}_g(s), \quad (12)$$

$$D' \hat{i}_g(s) + I_g \hat{d}'(s) = SC \hat{v}_0(s) + \frac{\hat{v}_0(s)}{R}. \quad (13)$$

The expression for the $\hat{v}_0(s)$ can be obtained from (13). Then, putting it in (12), we can obtain the expression of the input current as follows

$$\hat{i}_g(s) = G_{ig}(s) \hat{v}_g(s) + G_{id}(s) \hat{d}(s). \quad (14)$$

Thus, the transfer function $G_{id}(s)$ that can be derived for the input current and duty cycle can be expressed as

$$G_{id}(s) = \frac{K_{id} \left(\frac{s}{w_2} + 1 \right)}{\frac{s^2}{w_0^2} + \frac{s}{Qw_0} + 1}, \quad (15)$$

where

$$K_{id} = \frac{2U_0}{R(1-D)^2} \quad w_2 = \frac{2}{RC},$$

$$w_0 = \frac{1-D}{\sqrt{LC}}, \quad Q = R(1-D)\sqrt{C/L}. \quad (16)$$

Here $G_{id}(s)$ represents the transfer function of the input current and duty cycle in the power stage of the bridgeless Cuk PFC circuit, and can be used as the control object during the analysis and design of the control circuit. The capacitance, resistance, and inductance in the transfer function expression are constant, so the duty cycle D and output voltage, V_0 change during the normal operation.

2.2. Single-cycle current control algorithm

The single-cycle control model [7] was introduced by Prof. Semdey from the California University, USA in the early 1990s. Single-cycle control method does not require multipliers, as a non-linear control technology, it has a dual function of control and regulation. The main idea of single-cycle control is: the average switch value in any switching cycle must be equal or proportional to its control reference by controlling the duty cycle of the switching tube. Thus, the advantage of the single-cycle control is that no matter whether the circuit is in a transient or a steady state during operation, it is possible to keep the average of the controlled quantity proportional to its given value. The disturbance on the power supply side is suppressed. In this control algorithm, the circuit will not produce the transient error and steady-state error during the entire process.

In the circuit design process, the use of single cycle control has the following advantages: constant switching frequency, faster dynamic response, strong anti-

jamming capability, and easy implementation. Therefore, many scholars will shift the focus of PFC research to single cycle control. Many scholars at home and abroad have done a lot of practical innovation in the field of single cycle control. The basic schematic diagram of the single cycle control algorithm is shown in Fig. 3.

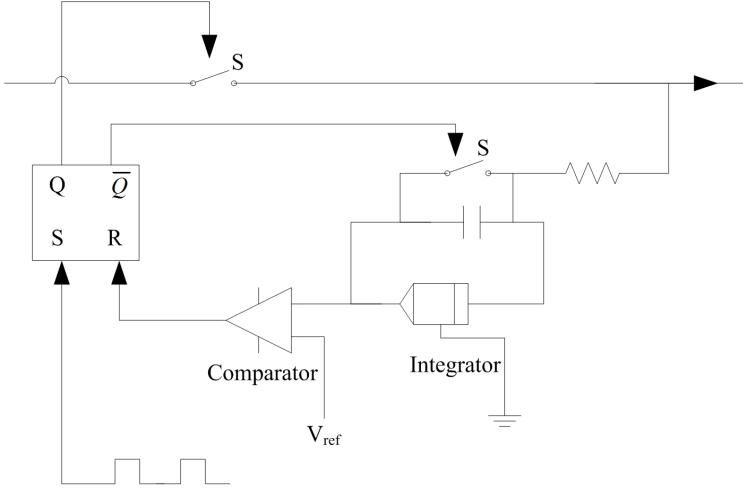


Fig. 3. Basic schematic diagram of single cycle control

The input signal of switch S is denoted by $x(t)$, and the output signal is denoted by $y(t)$. Assuming that the turn-on time in any switching cycle is T_{on} , the turn-off time is T_{off} and T_s is a complete switching period, then the duty cycle is $d = T_{on}/T_s$. The circuit operates at a constant switching frequency $f_s = 1/T_s$. Through the previous analysis we can know that the purpose of single cycle control is to adjust the breakover time T_{on} of the switch S. Through the adjustment of the breakover time, the average value of output $y(t)$ is equal to the reference value V_{ref} , so that the elimination of transient and steady-state errors is achieved. The operation of the integrator is achieved by controlling the on-off of the switch S by a CLOCK having a fixed frequency, and the integral value of the integrator is as follows

$$V_{int} = \frac{1}{T_s} \int_0^{T_s} x(t) dt, \quad (17)$$

where $T_s = C_{int}R_{int}$ is the integral time constant (switching cycle).

In any one switching cycle, when the integrator value V_{int} and reference voltage V_{ref} are equal, the comparator output flips, RS flip-flop resets, and then the switch signal will be low so that the switch S turns off. The integrator resets and waits for the next switching cycle. If the output of the switch $y(t)$ in each cycle can be made equal to the integral value of the given reference value V_{ref} by modulating the duty

cycle of the switch, it can be expressed as follows

$$\int_0^{T_{\text{on}}} x(t) dt = \int_0^{T_s} V_{\text{ref}}(t) dt. \quad (18)$$

Simultaneously dividing T_s at both ends of the above equation yields an average of the output signal in each cycle which equals to the average of the given reference values

$$\frac{1}{T_s} \int_0^{T_s} x(t) dt = \frac{1}{T_s} \int_0^{T_s} V_{\text{ref}}(t) dt. \quad (19)$$

Then the average value of the output signal in the current switching cycle is

$$\bar{y}(t) = \frac{1}{T_s} \int_0^{T_{\text{on}}} x(t) dt = \frac{1}{T_s} \int_0^{T_s} V_{\text{ref}}(t) dt = V_{\text{ref}}, \quad (20)$$

so that

$$\bar{y}(t) = V_{\text{ref}}(t). \quad (21)$$

In the case of stable output, the output voltage is represented by U_0 . The input current changes in same phases and same frequency following the input voltage, which is the target of the PFC. The circuit is purely resistive to the grid and can be expressed as R_e , so that

$$i_L = \frac{U_{\text{in}}}{R_e}. \quad (22)$$

For Boost PFC, the input voltage U_{in} and output voltage U_0 exhibit the following relationship

$$\frac{U_0}{U_{\text{in}}} = \frac{1}{1-D}. \quad (23)$$

Here D is the duty cycle, and the conditions that the governing equations need to satisfy can be derived by using the input equation for the unity power factor in the ideal state. From (21) and (22) we can find

$$R_e i_L = U_0(1-D). \quad (24)$$

If R_s is the sampling resistance in the bridgeless PFC, (23) provides

$$R_s i_L = \frac{R_s}{R_e} U_0(1-D). \quad (25)$$

From the above formula we can see that the average output value U_0 and input U_{in} are not related to each other. The average value $\bar{y}(t)$ of the output signal can be made equal to the reference value V_{ref} in the current switching cycle once the single-cycle control is used, and irrespective of the input signal U_{in} is constant or fluctuating. In other words, a non-linear branch in the single-cycle control can be turned into a linear branch.

The single-cycle control technology has the following advantages:

1. The realization of the circuit is simple.
2. The total harmonic distortion of the grid current is small.
3. The control loop is not sensitive to noise interference
4. Direct output voltage is smooth, the adjustment range is very large.
5. The control loop is stable and has good dynamic response

Therefore, the technology of single cycle control is also called the instantaneous value control technique of switching voltage. It can suppress the disturbance of the input side signal $x(t)$ and disturbance of the load side and output signal $y(t)$ is very well, so as to ensure that the output voltage is constant.

3. Simulation verification and analysis

3.1. Single cycle control simulation

Set the model parameters: AC input voltage is $220 \sin(50t)$, the rated load is the ideal load 100Ω .

According to the principle of single cycle control, the system simulation model is obtained. The inductor size is $L = 1.5 \text{ mH}$, the input filter capacitance is $C = 1 \mu\text{F}$, the filter inductor is $L1 = 1 \mu\text{H}$, and the output filter capacitor is $C1 = 660 \mu\text{F}$. $R1$ and $R2$ are the sampling resistors of the direct current side, and $R1$ is much higher than $R2$. The PID parameters of the voltage loop are: $p = 5$, $i = 0.5$, the parameters of the current loop PID are $p = 30$, $i = 0.1$, and the output voltage is 400 V .

Single-cycle control simulation: the waveform of the input current and output voltage under the ideal state are shown in Fig. 4.

3.2. Charging pile overall circuit simulation

From simulation waveform under the single cycle control algorithm, it can be obtained a more smooth output voltage waveform, and the overshoot is less than 1% . In the single cycle control algorithm, the output load increases by 30% fluctuations, and changes from the original 100Ω into 130Ω . The resulting waveform is shown in Fig. 5.

4. Conclusion

We firstly analyzed the circuit model of bridgeless Boost PFC in order to obtain the transfer function of duty cycle and input current in the circuit. Then, the single cycle control algorithm in bridgeless PFC control algorithm was introduced, used for carrying out the simulation experiment. The simulation results of single cycle control algorithm are analyzed under the condition of input voltage fluctuation and

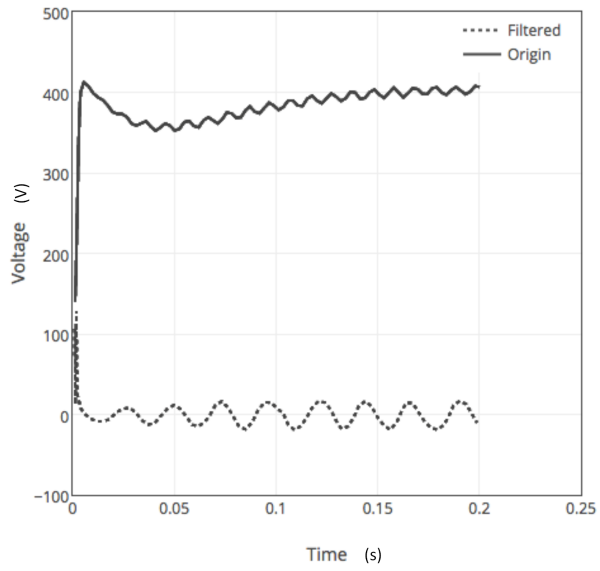


Fig. 4. Waveform obtained under single cycle control

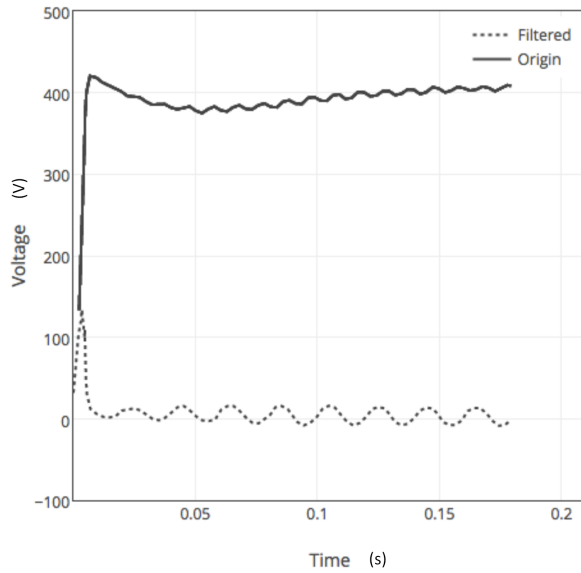


Fig. 5. Waveform of load fluctuation under single cycle control algorithm

load fluctuation. The single cycle control algorithm is applied to the whole circuit of the charging pile, and its feasibility is proved by simulation.

References

- [1] G. M. WALLER, E. D. WILLIAMS, S. W. MATTESON, T. A. TRABOLD: *Current and theoretical maximum well-to-wheels exergy efficiency of options to power vehicles with natural gas*. Applied Energy 127 (2014), 55–63.
- [2] E. FIGENBAUM, M. KOLBENSTVEDT, B. ELVEBAKK: *Electric vehicles – environmental, economic and practical aspects: As seen by current and potential users*. TOI Institute of Transport Economics Norwegian Centre for Transport Research, Report 1329, 2014.
- [3] Z. DARABI: *Impact of plug-in hybrid electric vehicles on the power grid in a smart environment*. Curtis Laws Wilson Library, Missouri University of Science and Technology, Doctoral Dissertation, 2012.
- [4] A. A. M. BENTO, A. R. C. D. SILVA: *Hybrid one-cycle controller for boost PFC rectifier*. IEEE Trans. Industry Applications 45 (2009), No. 1, 268–277.
- [5] G. CHEN, K. M. SMEDLEY: *Steady-state and dynamic study of one-cycle-controlled three-phase power-factor correction*. IEEE Trans. Industrial Electronics 52 (2005), No. 2, 355–362.
- [6] M. M. JOVANOVIĆ, Y. JANG: *State-of-the-art, single-phase, active power-factor-correction techniques for high-power applications - an overview*. IEEE Trans. Industrial Electronics 52 (2005) No. 3, 701–708.
- [7] A. J. SABZALI, E. H. ISMAIL, M. A. AL-SAFFAR, A. A. FARDOUN: *New bridgeless DCM SEPIC and CUK PFC rectifiers with low conduction and switching losses*. IEEE Trans. Industry Applications 47 (2011), No. 2, 873–881.

Received November 16, 2016